An arbitrary order differentiator design paradigm with adaptive gains

Markus Reichhartinger[a] and Sarah Spurgeon[b]

[a]Institute of Automation and Control, Graz University of Technology, 8010 Graz, Austria; [b] Department of Electronic & Electrical Engineering, University College London, London WC1E 7JE, UK

ARTICLE HISTORY
Compiled December 8, 2017

ABSTRACT
Higher order sliding mode differentiators have received a great deal of attention in the literature. For the case of reconstructing the first derivative, theoretical convergence conditions for the differentiator are available from which differentiator parameters may be selected. For the case of higher order derivatives, some parameter settings have been suggested for differentiators of certain order but there is no tuning algorithm available to determine convergent parameters for differentiators of arbitrary order. Whilst recognising the strong theoretical properties of sliding mode differentiators, practitioners report difficulties in achieving wide envelope performance from a single set of differentiator parameters. This paper proposes a constructive design paradigm to generate differentiator parameters which is seen to provide a natural framework to facilitate simple on-line adaptation of the chosen gains. Simulation experiments as well as experimental results are presented to demonstrate the proposed approach.

KEYWORDS
arbitrary order differentiator, sliding mode, adaptive gains

1. Introduction

The robust exact differentiator (RED) is a special case of the super-twisting algorithm. Stability considerations, robustness properties and convergence time estimates based on Lyapunov functions have been proposed in Davila, Moreno, and Fridman (2009); J. Moreno (2009); J. Moreno and Osorio (2008, 2012); Orlov, Aoustin, and Chevallereau (2011); Polyakov and Poznyak (2009). In this paper the RED is represented by a so-called pseudo-linear system Banks and Mhana (1992); Langson and Alleyne (1999, 2002) which motivates the development of a new tuning procedure which will be seen to provide a natural framework to adapt the gains of the differentiator to accommodate varying signal characteristics. Initially, the unperturbed case is studied. State-dependent eigenvalues which guarantee vanishing estimation errors are described. Robustness of the differentiator is demonstrated exploiting existing convergence proofs.

Differentiators obtaining time-derivatives of an arbitrary order n are often based

Email: markus.reichhartinger@tugraz.at

on the ideas of higher-order sliding mode techniques which generate an exact result within finite-time Levant (2003); Y. Shtessel, Edwards, Fridman, and Levant (2014); Y. B. Shtessel, Moreno, Plestan, Fridman, and Poznyak (2010). This requires a noise-free signal to be differentiated and a known Lipschitz constant of its n^{th} time-derivative. The latter requirement may be relaxed by the implementation of adaptive gains differentiators. This strategy is available for the general order case in Sidhom, Pham, Thvenoux, and Gautier (2010); Sidhom, Smaoui, Thomasset, Brun, and Bideaux (2011). For the first order case a number of solutions are known from the literature Kobayashi and Furuta (2007); Y. Shtessel, Taleb, and Plestan (2012). The authors Oliveira, Estrada, and Fridman (2015, 2016) propose a higher order sliding mode differentiator with dynamic gains in the context of output feedback control where the gains are scaled using a function which depends on the input signal of the system and a norm bound of the estimated state variables in combination with some constants related to worst-case estimation of the absolute value of the desired time derivative of the output signal of the system. Although this function includes parameters and signals which may not be available in the scenario considered in this paper, the structure of the differentiator is similar to the adaptive differentiator discussed in this paper.

In the case of constant gains, differentiation algorithms of a fixed certain order are available. They mainly provide the first or more rarely the second derivative, see e.g. Ortiz-Ricardez, Sanchez, and Moreno (2015). The well-known first-order sliding mode differentiator is enhanced in Cruz-Zavala, Moreno, and Fridman (2011) to provide the exact derivative within a prescribed time independent of the initial conditions of the differentiation algorithm. A differentiator which relies on a discontinuous high-gain observer is outlined in Orani, Pisano, and Usai (2006) where a discrete-time implementation is also discussed. An example of the arbitrary-order differentiator presented in Levant (2003) for the computation of the first and second derivative is given in Pisano and Usai (2011).

2. Robust exact differentiator - constant gains

A RED provides an output signal ν which exactly coincides with the first time derivative of the noise-free input signal $f(t)$, i.e. the difference $f^{(1)} - \nu$ tends to zero after a finite transient time and remains there. The only assumption required is that the 2^{nd} derivative w.r.t. time t of the input signal $f(t)$, i.e. $f^{(2)}(t)$, satisfies

$$\left| \frac{d^2 f}{dt^2} \right| \leq L, \tag{1}$$

where L denotes the finite and known Lipschitz constant. This differentiator is robust to uncertainties in the input signal f which satisfy inequality (1). The differentiator can be regarded as the closed-loop system obtained by the application of the super-twisting algorithm as control law such that the state z_0 tracks the function f where the RED may be represented by

$$\frac{dz_0}{dt} = \kappa_0 \lfloor f - z_0 \rceil^{\frac{1}{2}} + z_1, \tag{2a}$$

$$\frac{dz_1}{dt} = \kappa_1 \operatorname{sign}(f - z_0), \tag{2b}$$

$$\nu = z_1, \tag{2c}$$

with the abbreviation

$$\lfloor a \rceil^b := |a|^b \operatorname{sign}(a), \quad a, b \in \mathbb{R}. \tag{3}$$

The positive constants κ_1 and κ_2 are the tuning parameters. The error dynamics is given by

$$\frac{dx_0}{dt} = x_1 - \kappa_0 \lfloor x_0 \rceil^{\frac{1}{2}}, \tag{4a}$$

$$\frac{dx_1}{dt} = -\kappa_1 \operatorname{sign}(x_0) + \frac{d^2 f}{dt^2}, \tag{4b}$$

where the estimation errors are

$$x_0 := f - z_0 \qquad \text{and} \qquad x_1 := \frac{df}{dt} - z_1. \tag{5}$$

Proper choice of the parameters κ_0 and κ_1 must ensure the convergence of the trajectories of (4) to zero in finite time despite the uncertainty (1).

2.1. *Overview of existing tuning procedures*

It is shown in Y. Shtessel et al. (2014) that any parameters satisfying

$$\kappa_1 > L \qquad \text{and} \qquad \kappa_0^2 > \frac{2\left(\kappa_1 + L\right)^2}{\kappa_1 - L} \tag{6}$$

yield global finite time stability of the origin of the system (4). Slightly different inequalities are proposed in Levant (1998):

$$\kappa_1 > L \qquad \text{and} \qquad \kappa_0^2 \geq 4L\frac{\kappa_1 + L}{\kappa_1 - L} \tag{7}$$

These result from a conservative estimate of the trajectories of (4). A further setting is available from Orlov et al. (2011) as

$$L < \min\left\{\frac{\kappa_0}{2}, \frac{\kappa_0\kappa_1}{1+\kappa_0}\right\}. \tag{8}$$

This setting is obtained by a Lyapunov function based approach where linear gains may be considered. Another tuning algorithm proposed in J. A. Moreno (2012) requires a feasible solution of the linear matrix inequality (LMI)

$$\begin{bmatrix} \mathbf{A}^{\mathrm{T}}\mathbf{P} + \mathbf{P}\mathbf{A} + \mathbf{c}L^2\mathbf{c}^{\mathrm{T}} & \mathbf{P}\mathbf{b} \\ \mathbf{b}^{\mathrm{T}}\mathbf{P} & -1 \end{bmatrix} < 0 \tag{9}$$

with a positive definite matrix $\mathbf{P} = \mathbf{P}^{\mathrm{T}} \in \mathbb{R}^{2\times 2}$,

$$\mathbf{A} := \begin{bmatrix} -\kappa_0 & 1 \\ -2\kappa_1 & 0 \end{bmatrix}, \mathbf{c} := \begin{bmatrix} 2 & 0 \end{bmatrix}^{\mathrm{T}} \text{ and } \mathbf{b} := \begin{bmatrix} 0 & 1 \end{bmatrix}^{\mathrm{T}}. \tag{10}$$

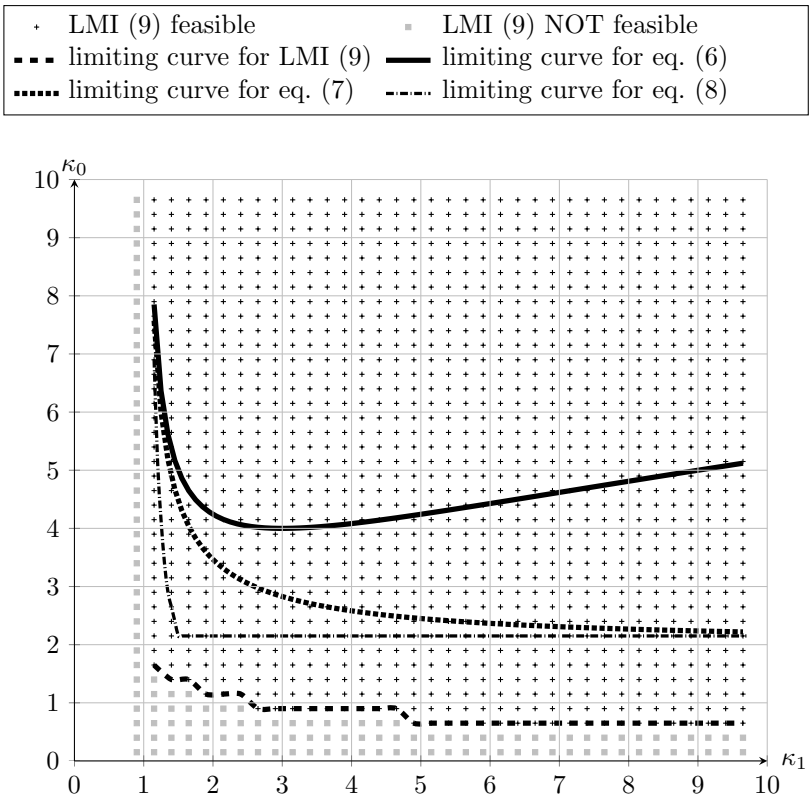

Figure 1.: The values of κ_0 and κ_1 obtaining a feasible solution of linear matrix inequality (LMI) given in (9) with $L = 1$ are indicated. Below the limit curves no valid setting w.r.t. the corresponding setting is available.

In Figure 1 valid regions of the presented inequalities are depicted for the case $L = 1$. Note that any valid setting of κ_0 and κ_1 for $L = 1$ may be generalized for general Lipschitz constants $\tilde{L}$ of $f^{(2)}$ using the scaled parameters $\tilde{\kappa}_0 = \kappa_0\sqrt{\tilde{L}}$ and $\tilde{\kappa}_1 = \kappa_1\tilde{L}$, see Y. Shtessel et al. (2014). In order to avoid overestimation of the gains of the RED, it is suggested in Levant (1998) that the parameters κ_0 and κ_1 are tuned based on numerical simulations rather than using the discussed inequalities. Practitioners have reported difficulties achieving theoretical performance levels for practical systems across a wide and uncertain envelope of operation. Within the area of haptics, for example, accurate and insensitive real time velocity estimation is required. The RED has been tested in both simulation and experimentally with application to passivity-based control of haptic displays in Chawda, Celik, and O'Malley (2011). The authors report that the performance of the RED was difficult to tune and it was found that low and high velocity signals may require different sets of optimized gains. This motivates the need to develop adaptive methods to tune the gains of the RED on-line.

2.1.1. An alternative interpretation of the tuning procedure

The adaptive gains differentiator developed in the subsequent sections will rely on a pseudo-linear representation of the discussed error dynamics (4) and is based on

eigenvalue considerations. Using

$$\operatorname{sign}(a) = \frac{a}{|a|}, \tag{11}$$

where $a = 0$ formally has to be excluded, and the function

$$\lfloor a \rceil^b = |a|^b \operatorname{sign}(a) = |a|^{b-1} a, \tag{12}$$

the error dynamics of the RED in (4) becomes

$$\frac{d\mathbf{x}}{dt} = \mathbf{M}(x_0)\mathbf{x} + \mathbf{b} f^{(2)}, \tag{13}$$

with $\mathbf{x} := \begin{bmatrix} x_0 & x_1 \end{bmatrix}^{\mathrm{T}}$ and

$$\mathbf{M}(x_0) := \begin{bmatrix} -\kappa_0 |x_0|^{-\frac{1}{2}} & 1 \\ -\kappa_1 |x_0|^{-1} & 0 \end{bmatrix}. \tag{14}$$

System (13) is a pseudo-linear system and all system properties of (4) are maintained.

Remark 1. This is the first time that a pseudo linear representation is used in the context of sliding mode based differentiators. It enables the construction of a systematic parameter tuning approach. Note that for differentiators of arbitrary order only simulation based tuning methods are available.

Remark 2. Results relating to pseudo-linear systems are also considered in the work of Langson and Alleyne (1999, 2002). However, the dynamic system under consideration in this paper does not have the smoothness properties required for the stability theorems within this work. Therefore, these theorems are not applied. It also should be noted that the results on pseudo-linear systems applied pertain to the case of local, not global, stability.

The characteristic polynomial of $\mathbf{M}(x_0)$ (almost everywhere) is given by

$$w(s) = s^2 + \kappa_0 |x_0|^{-\frac{1}{2}} s + \kappa_1 |x_0|^{-1}. \tag{15}$$

It can be shown that the roots $p_1, p_2 \in \mathbb{C}$ of equation (15) are given by

$$s_1(x_0) = |x_0|^{-\frac{1}{2}} p_1 \quad \text{and} \quad s_2(x_0) = |x_0|^{-\frac{1}{2}} p_2, \tag{16}$$

so that equation (15) may be expressed as

$$w(s) = s^2 - |x_0|^{-\frac{1}{2}} (p_1 + p_2) s + |x_0|^{-1} p_1 p_2. \tag{17}$$

Comparing (15) and (17) and equating coefficients

$$\kappa_1 = p_1 p_2 \quad \text{and} \quad \kappa_0 = -(p_1 + p_2) \tag{18}$$

and a mapping between the parameters of the RED and the free parameters p_1 and p_2 is established.

Remark 3. Note that the parametrization (18) is not limiting but is an alternative representation of the usual sliding mode differentiator which is practically motivated.

Using (16) and (18), matrix $\mathbf{M}(x_0)$ in (14) becomes

$$\mathbf{M}(x_0) = \begin{bmatrix} s_1 \left(1 + \frac{p_2}{p_1}\right) & 1 \\ -s_1^2 \frac{p_2}{p_1} & 0 \end{bmatrix}. \tag{19}$$

The first theorem motivates RED parameter selections based on this approach in the unperturbed case, i.e. $f^{(2)} = 0$.

Theorem 2.1. *Select the roots p_1 and p_2 such that the polynomial $\bar{w}(p) = p^2 + \kappa_0 p + \kappa_1$ is Hurwitz. Then the matrix $\mathbf{M}(x_0)$ is a stable matrix, i.e.*

$$\Re\{s_k\} < 0 \qquad \forall x_0(t) \qquad k = 1, 2 \tag{20}$$

and furthermore the origin of system (13)*, i.e. $x_0 = x_1 = 0$, with the matrix $\mathbf{M}(x_0)$ given in equation* (19) *and $f^{(2)} = 0$ is globally finite time stable with the parameter setting given in equation* (18)*.*

The proof of Theorem 2.1 is given in the appendix.

Remark 4. The proof of Theorem 2.1 exploits the homogeneity properties of system (13) as outlined in Bacciotti and Rosier (2005); Levant (2005). It should be noted that there are other options for proving the finite time convergence of the estimation errors x_0 and x_1. In Levant (1998), the proof is based on geometrical considerations of the closed-loop trajectories and in J. Moreno and Osorio (2008), a Lyapunov function is used. Also note that in general all characteristics of the differentiator are maintained. This naturally also includes the well-documented behaviour in the case of noisy and sampled input signals as outlined in Livne and Levant (2014).

The unperturbed case assumed in Theorem 2.1 motivates choosing the parameters κ_0 and κ_1 such that the polynomial $\bar{w}$ is Hurwitz. In order to ensure robustness w.r.t. the uncertainty given by inequality (1) the necessary condition for the existence of a sliding mode at the equilibrium point $x_0 = x_1 = 0$ given by

$$\kappa_1 = p_1 p_2 > L \tag{21}$$

has to be satisfied. The next Theorem shows that in the case of real roots p_1 and p_2 condition (21) is sufficient for asymptotic stability of the origin of system (13).

Theorem 2.2. *Select negative real roots p_1 and p_2 such that $p_1 p_2 > L$. Then the origin of system* (13) *is finite time stable with the parameters of the RED selected as given in equation* (18)*.*

The proof of Theorem 2.2 is presented in the appendix. From Theorem 2.2 it also

follows that the parameters of the RED may be selected as

$$\kappa_1 > L \qquad \text{and} \qquad \kappa_0 \geq 2\sqrt{\kappa_1}, \tag{22}$$

which ensures real roots p_1 and p_2 of the polynomial $\bar{w}(s)$. It is interesting to consider complex roots, i.e. $p_1, p_2 \in \mathbb{C}$, which are obtained when $2\sqrt{\kappa_1} > \kappa_0$. From the proof of Theorem 2.2, finite time convergent estimation errors x_0 and x_1 can be ensured if

$$||G(s)||_\infty = \frac{4}{\kappa_0\sqrt{8\kappa_1 - \kappa_0^2}} < \frac{1}{L} \tag{23}$$

holds, which ensures feasibility of the LMI (9). In the case of complex roots a parameter setting is suggested by the following theorem.

Theorem 2.3. *Inequality* (23) *is satisfied in the case of complex roots* p_1, p_2 *by the choice of parameters*

$$\kappa_1 > L \quad \textit{and} \quad 2\sqrt{\kappa_1 - \sqrt{\kappa_1^2 - L^2}} < \kappa_0 < 2\sqrt{\kappa_1}. \tag{24}$$

The proof of Theorem 2.3 is given in the appendix. Note that the upper bound on the parameter κ_0 ensures complex roots and can be omitted in the case of real roots. Assume that κ_1 is selected so that $\kappa_1 = p_1 p_2 > L$. Use the following metric

$$d^2 := \kappa_1^2 - L^2 = (p_1 p_2)^2 - L^2 \tag{25}$$

and select κ_0 such that equation (90) from the proof of Theorem 2.3 holds, i.e.

$$\kappa_0 = 2\sqrt{\kappa_1 - d}, \tag{26}$$

the roots p_1 and p_2 of the polynomial $p^2 + p\kappa_0 + \kappa_1$ are given by

$$p_{1,2} = -\sqrt{\kappa_1 - d} \pm j\sqrt{d}. \tag{27}$$

Since κ_0 is selected such that (90) holds, inequality (23) will not be satisfied. This will be achieved by further increasing κ_0, which will reduce $|\Im\{p_{1,2}\}|$. Hence, in the case of complex conjugate roots, the absolute value of the imaginary part must satisfy

$$|\Im\{p_{1,2}\}| < \sqrt{d}. \tag{28}$$

Hence, the imaginary part of the roots may be increased whenever the distance d is increased which indicates a conservative choice of κ_1. The tuning procedure is summarized as follows:

(1) Select p_1, p_2 such that $p_1 p_2 > L$.
(2) In the case of complex roots the imaginary part must satisfy

$$|\Im\{p_1\}| < \left(\kappa_1^2 - L^2\right)^{\frac{1}{4}} = \left[(p_1 p_2)^2 - L^2\right]^{\frac{1}{4}},$$

where $\Re\{.\}$ and $\Im\{.\}$ denote the real and imaginary part of the corresponding roots.

3. Robust exact differentiator - adaptive gains

This eigenvalue based tuning procedure will now be extended in order to achieve vanishing estimation errors in the case of an unknown Lipschitz constant L. The idea is based on an appropriate online-scaling of the eigenvalues given in equation (16) using an additional strictly positive, time-varying parameter $\gamma(t)$. Therefore, the differentiator should be enhanced such that the eigenvalues are given by

$$\lambda_i(x_0) = \gamma(t)|x_0|^{-\frac{1}{2}} p_i = \gamma(t) s_i(x_0). \tag{29}$$

This can be realized by the modification of the applied super twisting algorithm such that the RED given in equation (2) becomes

$$\frac{dz_0}{dt} = \kappa_0\, \gamma(t)\, \lfloor f - z_0 \rceil^{\frac{1}{2}} + z_1, \tag{30a}$$

$$\frac{dz_1}{dt} = \kappa_1\, \gamma^2(t)\, \mathrm{sign}(f - z_0), \tag{30b}$$

$$\nu = z_1, \tag{30c}$$

which yields the corresponding error dynamics

$$\frac{d}{dt}\begin{bmatrix} x_0 \\ x_1 \end{bmatrix} = \begin{bmatrix} -\kappa_0\gamma|x_0|^{-\frac{1}{2}} & 1 \\ -\kappa_1\gamma^2|x_0|^{-1} & 0 \end{bmatrix}\begin{bmatrix} x_0 \\ x_1 \end{bmatrix} + \begin{bmatrix} 0 \\ 1 \end{bmatrix}\frac{d^2 f}{dt^2}. \tag{31}$$

A straightforward computation of the eigenvalues of the dynamic matrix involved in (31) verifies that its eigenvalues are given by $\lambda_i(x_0)$ as specified in equation (29). Note, that the eigenvalues λ_i and s_i have the same sign and consequently the same tuning procedure as outlined in Section 2.1.1 may be applied. Hence the constant gains κ_0 and κ_1 can be selected such that the polynomial $\bar{w}(p)$ given in Theorem 2.1 is Hurwitz. In terms of the robustness against the unknown but bounded function $\frac{d^2 f}{dt^2}$ it becomes evident from Theorem 2.2 that

$$\kappa_1\gamma^2 = p_1 p_2 \gamma^2 > L \tag{32}$$

has to be satisfied in the case of real roots. The idea of the proposed gain adaptation therefore is to increase the variable γ such that the estimation errors vanish and consequently inequality (32) has to be satisfied. Using equation (18), the error dynamics (31) may be written as

$$\frac{d}{dt}\begin{bmatrix} x_0 \\ x_1 \end{bmatrix} = \begin{bmatrix} \lambda_1(x_0)\left(1 + \frac{p_2}{p_1}\right) & 1 \\ -\frac{p_2}{p_1}\lambda_1^2(x_0) & 0 \end{bmatrix}\begin{bmatrix} x_0 \\ x_1 \end{bmatrix} + \begin{bmatrix} 0 \\ 1 \end{bmatrix}\frac{d^2 f}{dt^2}. \tag{33}$$

To derive an adaptation mechanism specifying the time behaviour of γ, consider the modified version of the Lyapunov function used in the proof of Theorem 2.1:

$$V(x_0, x_1, \gamma) = \gamma^2 |x_0| + \frac{1}{2p_1 p_2} x_1^2, \tag{34}$$

where positive definiteness is ensured by an appropriate selection of the real, strictly negative constants p_1 and p_2. The time derivative of V along the trajectories of system (33) in the case $\frac{d^2 f}{dt^2} = 0$ yields

$$\frac{dV}{dt} = \gamma^2 \lambda_1(x_0) \left(1 + \frac{p_2}{p_1}\right) |x_0| + 2\gamma \frac{d\gamma}{dt} |x_0|. \tag{35}$$

In order to ensure negative semidefiniteness of $\frac{dV}{dt}$ by the design of an adaptation algorithm $\frac{d\gamma}{dt}$ the first term in equation (35) is rewritten using (16) and (18) to yield

$$\frac{dV}{dt} = -\gamma^3 \kappa_0 |x_0|^{\frac{1}{2}} + 2\gamma \frac{d\gamma}{dt} |x_0|. \tag{36}$$

Using the adaptation law

$$\frac{d\gamma}{dt} = \frac{\gamma}{2} \alpha \cdot \begin{cases} |x_0|^{-\frac{1}{2}} & \text{for} \quad |x_0| \geq 1 \\ |x_0| & \text{for} \quad |x_0| < 1 \end{cases} \qquad \text{with} \qquad \gamma(t=0) = 1, \tag{37}$$

where the constant tuning parameter α is selected as

$$0 < \alpha < \kappa_0 \tag{38}$$

generates

$$\frac{dV}{dt} = -\gamma^2 \cdot \begin{cases} |x_0|^{\frac{1}{2}} (\gamma \kappa_0 - \alpha) & \text{for} \quad |x_0| \geq 1 \\ \gamma \kappa_0 |x_0|^{\frac{1}{2}} - \alpha x_0^2 & \text{for} \quad |x_0| < 1 \end{cases}. \tag{39}$$

The initial value $\gamma(0) = 1$, the selection of the tuning parameter α according to inequality (38) and the design of the adaptation algorithm as stated in (37) ensure negative semidefiniteness of $\frac{dV}{dt}$ for any x_0. Due to the assumption $\frac{d^2 f}{dt^2} = 0$, system (33) represents an autonomous discontinuous system and the extended version of the Invariance Principle as outlined in Orlov (2009) is applicable. The radial unboundedness of V, the fact that the largest invariant subset of the manifold where $\frac{dV}{dt} = 0$ is characterized by $x_0 = x_1 = 0$ and a constant value of γ and that $\gamma \geq 1$ shows that that all the trajectories of system (33) vanish asymptotically.

Remark 5. The adaptation law given in equation (37) is designed such that negative semidefiniteness of $\frac{dV}{dt}$ is guaranteed. The design is based on the idea that "large" deviations from $x_0 = 0$, which may occur initially, should not generate arbitrarily fast adaptation of γ. Also "small" deviations, i.e. $x_0 \approx 0$, should not lead to an unbounded

adaptation rate. This is apparent from the characteristics

$$\lim_{|x_0|\to\infty} \frac{d\gamma}{dt} = \lim_{|x_0|\to 0} \frac{d\gamma}{dt} = 0. \tag{40}$$

The adaptation law guarantees robustness against a bounded second time derivative of f. The origin of system (33) is an equilibrium whenever (32) is satisfied. Hence, γ is increased by the adaptation law (37) until $x_0 = 0$ is maintained and consequently inequality (32) holds.
In the case of an input signal $f(t)$ which is corrupted by noise of maximum amplitude ε a modified version of the adaptation algorithm given in equation (37) is proposed as

$$\frac{d\gamma}{dt} = \frac{\gamma}{2}\alpha \cdot \begin{cases} |x_0|^{-\frac{1}{2}} & \text{for} \quad |x_0| \geq 1 \\ |x_0| & \text{for} \quad |x_0| < 1 \\ 0 & \text{for} \quad |x_0| < 1.1\varepsilon \end{cases} \qquad \text{with} \qquad \gamma(0) = 1. \tag{41}$$

Here adaptation is halted whenever the domain $|x_0| < 1.1\varepsilon$ is reached by the differentiator. It is obvious that due to noise the estimation error x_1 will not vanish and it is well-known that it is proportional to $\sqrt{\varepsilon}$, see Levant (1998). If there is a domain of x_1 introduced such that the adaptation is halted then also adaptation laws have been designed in literature which also allow γ to be reduced, see Plestan, Shtessel, Bregeault, and Poznyak (2010); Y. Shtessel et al. (2012). A modified version of the adaptation algorithm given by

$$\frac{d\gamma}{dt} = \frac{\gamma}{2}\alpha \cdot \begin{cases} |x_0|^{-\frac{1}{2}} & \text{for} \quad |x_0| \geq 1 \\ |x_0| & \text{for} \quad |x_0| < 1 \\ \frac{1}{\gamma} - 1 & \text{for} \quad |x_0| < 1.1\varepsilon \end{cases} \qquad \text{with} \qquad \gamma(0) = 1, \tag{42}$$

also provides the ability to reduce γ whenever the estimation error x_0 belongs to the prespecified boundary layer of width 1.1ε. Applying this modified version of the adaptation algorithm, convergence to the origin $x_0 = x_1 = 0$ cannot occur. This is known from other adaptive techniques using a boundary layer in order to facilitate gain reduction, see Plestan et al. (2010); Y. Shtessel et al. (2012).

Remark 6. In the case of the adaptation law (42) and $|x_0| \leq 1.1\varepsilon$, the adaptation parameter γ is governed by

$$\frac{d\gamma}{dt} = -\frac{\gamma\alpha}{2} + \frac{\alpha}{2} \tag{43}$$

and the unique equilibrium point of equation (43) characterized by

$$0 = -\frac{\gamma_e\alpha}{2} + \frac{\alpha}{2} \tag{44}$$

is given by $\gamma_e = 1$. Hence, the adaptation parameter γ will not converge towards values below 1. The adaptive gain differentiator therefore may compensate for unknown Lipschitz constants L in the case of underestimated differentiator parameters κ_0 and κ_1. It, however, does not reduce these parameters in the case of their overestimation.

Remark 7. Assume that the estimation error converges so that $|x_0| \leq 1.1\varepsilon$ holds. In this case the Lyapunov function is given by

$$\frac{dV}{dt} = -\gamma^3 \kappa_0 |x_0|^{\frac{1}{2}} - \gamma\alpha|x_0| \left(\gamma - 1\right) \tag{45}$$

which is negative semi-definite since $\gamma \geq 1 \ \forall t \geq 0$. It becomes evident that this adaptive gains differentiator is derived using a Lyapunov function assuming $\frac{d^2 f}{dt^2} = 0$. The time-derivative of the Lyapunov function given in equation (45) is negative, however, γ may be reduced such that inequality (32) is no longer satisfied. Consequently the estimation error x_0 will leave the boundary layer specified by $|x_0| \leq 1.1\varepsilon$ and the adaptation will start again by increasing the parameter γ.

4. Arbitrary-order robust exact differentiator - adaptive gains

The adaptive tuning procedure of the first-order robust exact differentiator will now be generalized for arbitrary-order differentiators. An n^{th}-order robust exact differentiator determines the first n time-derivatives of a signal $f(t)$ which satisfies

$$\left| \frac{d^{n+1}}{dt^{n+1}} f(t) \right| \leq L, \tag{46}$$

where L again denotes the Lipschitz constant, however, in the general order case it denotes the Lipschitz constant of the n^{th}-time derivative. The implementation of the non-recursive adaptive gain differentiator

$$\frac{dz_i}{dt} = z_{i+1} + \kappa_i \gamma^{i+1} \left\lfloor f - z_0 \right\rceil^{\frac{n-i}{n+1}} \qquad \text{with} \qquad z_{n+1} := 0 \qquad \text{and} \qquad i = 0, 1, \ldots, n \tag{47}$$

and the definition of the errors $x_i := \frac{d^i}{dt^i} f - z_i$ yields the differential equations

$$\frac{dx_k}{dt} = x_{k+1} - \kappa_k \gamma^{k+1} \left\lfloor x_0 \right\rceil^{\frac{n-k}{n+1}}, \qquad k = 0, 1, \ldots n-1, \tag{48a}$$

$$\frac{dx_n}{dt} = \frac{d^{n+1}}{dt^{n+1}} f - \kappa_n \gamma^{n+1} \operatorname{sign}(x_0), \tag{48b}$$

describing the estimation error dynamics. The constant tuning parameters are denoted by κ_i and may be selected based on the ideas of Theorem 2.1. The time-varying adaptation parameter γ will be governed by the adaptation law presented in equation (37) and, in the case of a function f corrupted by noise, by equation (41) or equation (42). Exploiting relation (12), the error dynamics from equations (48) represented as

a pseudo linear system yield

$$\frac{d\mathbf{x}}{dt} = \begin{bmatrix} -\kappa_0\gamma|x_0|^{-\frac{1}{n+1}} & 1 & 0 & \dots & 0 \\ -\kappa_1\gamma^2|x_0|^{-\frac{2}{n+1}} & 0 & 1 & \ddots & 0 \\ \vdots & \vdots & \ddots & \ddots & \vdots \\ -\kappa_{n-1}\gamma^n|x_0|^{-\frac{n-1}{n+1}} & 0 & 0 & \dots & 1 \\ -\kappa_n\gamma^{n+1}|x_0|^{-1} & 0 & 0 & \dots & 0 \end{bmatrix} \mathbf{x} + \begin{bmatrix} 0 \\ 0 \\ \vdots \\ 0 \\ 0 \\ 1 \end{bmatrix} \frac{d^{n+1}}{dt^{n+1}} f \tag{49}$$

$$=: \mathbf{M}(x_0, \gamma)\mathbf{x} + \mathbf{b}\frac{d^{n+1}}{dt^{n+1}} f, \tag{50}$$

where the errors x_i were composed by the vector

$$\mathbf{x} := \begin{bmatrix} x_0 & x_1 & \dots & x_n \end{bmatrix}^{\mathrm{T}}. \tag{51}$$

The determinant of the matrix $\mathbf{M}$ can easily be computed and represented as

$$\det \mathbf{M}(x_0, \gamma) = (-\gamma)^{n+1}\kappa_n|x_0|^{-1} = \prod_{i=1}^{n+1} p_i\gamma|x_0|^{-\frac{1}{n+1}}. \tag{52}$$

The characteristic polynomial of $\mathbf{M}$ is given by

$$\Delta(s) = s^{n+1} + \kappa_0\gamma|x_0|^{-\frac{1}{n+1}}s^n + \kappa_1\gamma^2|x_0|^{-\frac{2}{n+1}}s^{n-1} + \ldots + \kappa_n\gamma^{n+1}|x_0|^{-1} \tag{53}$$

and the representation of the determinant of $\mathbf{M}$ in equation (52) motivates the structure of the eigenvalues of the matrix $\mathbf{M}$ as

$$\lambda_i(x_0, \gamma) = \gamma p_i|x_0|^{-\frac{1}{n+1}}. \tag{54}$$

Using these eigenvalues λ_i in the characteristic polynomial (53), i.e.

$$\Delta(\lambda_i(x_0, \gamma)) = \gamma^{n+1}|x_0|^{-1}\left(p_i^{n+1} + \kappa_0 p_i^n + \kappa_1 p_i^{n-1} + \ldots + \kappa_n\right), \tag{55}$$

it becomes evident that the eigenvalues are given by (54). The tuning parameters κ_i of the differentiator are selected such that the polynomial

$$\bar{w}(p) = p^{n+1} + \kappa_0 p^n + \kappa_1 p^{n-1} + \ldots + \kappa_n \tag{56}$$

is Hurwitz and consequently $\Delta(\lambda_i) = 0$ holds. Furthermore, this tuning procedure implies, that all eigenvalues λ_i are negative[1] and the matrix $\mathbf{M}$ is stable. The robustness against the perturbation $\frac{d^{n+1}}{dt^{n+1}}f$ of an arbitrary-order differentiator is assumed to be achieved by the same approach as discussed in Section 2 in the first-order case. Hence, focusing on the $(n+1)^{\text{th}}$ differential equation describing the error dynamics, i.e.

$$\frac{dx_n}{dt} = \frac{d^{n+1}}{dt^{n+1}} f - \kappa_n\gamma^{n+1}\,\mathrm{sign}(x_0), \tag{57}$$

[1]Note that in this article complex roots are not considered.

reveals a necessary condition for vanishing error variables given by

$$\kappa_n \gamma^{n+1} > L. \tag{58}$$

Note that this inequality requires that

$$\left| \prod_{i=1}^{n+1} p_i \gamma \right| = \gamma^{n+1} \left| \prod_{i=1}^{n+1} p_i \right| > L, \tag{59}$$

see equation (52). Hence, in the case of convergent estimation error variables, the absolute value of the product of the roots of the polynomial $\bar{w}(p)$ in combination with the adaptation algorithm (37), (41) or (42) ensures that inequality (58) is satisfied after an initial transient time.

Remark 8. The order of the adaptation law in the differentiator is independent of the order of the differentiator; the order of the adaptation law is always 1. Implementation of the proposed differentiator requires a constant gains differentiator implementation to be augmented by the γ-dynamics. The existing parameters κ_i can remain.This is in contrast to the scheme proposed in Sidhom et al. (2011), where each differentiator parameter requires an additional differential equation in the adaptation scheme.

Remark 9. Note that in order to avoid overestimation of the gains, the adaptation algorithm as given in equation (42) may also be implemented. This concept was realized in the simulation scenario 3, see Section 5.3 where the performance of the proposed strategy in the case of an input signal corrupted by noise is investigated.

4.1. *A remark on the parameter tuning of arbitrary-order differentiators with constant gains.*

The arbitrary-order differentiator is now considered when the Lipschitz constant L is known. This can provide the initial differentiator parameters κ_i required by the proposed adaptive gain differentiator. In the case of known constant L, adaptation is not required and γ can be assumed to be constant. Assume $\gamma = 1$. The non-recursive differentiator becomes

$$\frac{dz_i}{dt} = z_{i+1} + \kappa_i \lfloor f - z_0 \rceil^{\frac{n-i}{n+1}} \quad \text{and} \quad z_{n+1} := 0, \tag{60}$$

with the output $\nu = z_n$. Hence, the differentiator given in Levant (2003) is recovered. The error dynamics is governed by

$$\begin{aligned}
\frac{dx_0}{dt} &= x_1 - \kappa_0 \lfloor x_0 \rceil^{\frac{n}{n+1}}, \\
\frac{dx_1}{dt} &= x_2 - \kappa_1 \lfloor x_0 \rceil^{\frac{n-1}{n+1}}, \\
&\vdots \\
\frac{dx_n}{dt} &= \frac{d^{n+1}f}{dt^{n+1}} - \kappa_n \operatorname{sign}(x_0),
\end{aligned} \tag{61}$$

This may be represented in the pseudo-linear representation given by equation (49), i.e.

$$\frac{d\mathbf{x}}{dt} = \mathbf{M}(x_0, 1)\mathbf{x} + \mathbf{b}\frac{d^{n+1}}{dt^{n+1}}f. \tag{62}$$

The eigenvalues of the matrix $\mathbf{M}(x_0, 1)$, which are given in equation (54), also may be selected such that the polynomial $\bar{w}(p)$ given in equation (56) solely has negative real roots, hence, the parameters κ_i are selected such that the matrix $\mathbf{M}(x_0, 1)$ is stable. It follows from (54) that

$$\lambda_i(x_0, 1) < 0 \qquad \forall x_0 \tag{63}$$

and

$$\lim_{x_0 \to 0} |\lambda_i(x_0, 1)| = \infty. \tag{64}$$

From equation (62) it becomes evident that in this section also the pseudo-linear system representation as used in Section 2 is exploited. As in the case of the differentiator of first order (see Remark 2), the matrix $\mathbf{M}$ does not satisfy the smoothness conditions required by the theorems presented by Langson and Alleyne (1999, 2002). Consequently its application is not valid. Any parameter setting of the differentiator which yields finite error convergence must satisfy $\kappa_n > L$, i.e. the inequality $\left|\prod_{i=1}^{n+1} p_i\right| > L$ holds, see equations (58) and (59). Hence, for the case of real roots p_i and motivated by the results of Section 2.1.1 the parameters κ_i of an n^{th}-order differentiator with constant gains may be tuned by the following paradigm:

(1) Select negative real roots p_i such that

$$\prod_{i=1}^{n+1} |p_i| = \alpha > L. \tag{65}$$

(2) Compute the parameters κ_i by equating the coefficients of the polynomial $\bar{w}(p)$,

i.e.

$$p^{n+1} + \kappa_0 p^n + \ldots + \kappa_n = \prod_{i=1}^{n+1} (s - p_i). \tag{66}$$

Whilst this paradigm is intuitive, there is currently no formal theoretical proof of convergence for differentiators of the form (49) with the setting (65) and (66), where system (49) is of order greater than 2. The obtained parameters can be applied to generate the parameters κ_i of an adaptive gain differentiator as previously discussed. It is desirable to generate small parameters κ_i, and in addition satisfy inequality (65). For differentiators up to order six, possible parameters are listed in Table 1. Note that currently no suggestions of convergent differentiator parameters for the case $n > 5$ are available. The parameters listed in Table 1 may be used as initial parameters to

Table 1.: Differentiator parameters up to order 6.

	κ_0	κ_1	κ_2	κ_3	κ_4	κ_5	κ_6
$n=1$	$2\alpha^{\frac{1}{2}}$	α					
$n=2$	$3\alpha^{\frac{1}{3}}$	$3\alpha^{\frac{2}{3}}$	α				
$n=3$	$4\alpha^{\frac{1}{4}}$	$6\alpha^{\frac{1}{2}}$	$4\alpha^{\frac{3}{4}}$	α			
$n=4$	$5\alpha^{\frac{1}{5}}$	$10\alpha^{\frac{2}{5}}$	$10\alpha^{\frac{3}{5}}$	$5\alpha^{\frac{4}{5}}$	α		
$n=5$	$6\alpha^{\frac{1}{6}}$	$15\alpha^{\frac{1}{3}}$	$20\alpha^{\frac{1}{2}}$	$15\alpha^{\frac{2}{3}}$	$6\alpha^{\frac{5}{6}}$	α	
$n=6$	$7\alpha^{\frac{1}{7}}$	$21\alpha^{\frac{2}{7}}$	$35\alpha^{\frac{3}{7}}$	$35\alpha^{\frac{4}{7}}$	$21\alpha^{\frac{5}{7}}$	$7\alpha^{\frac{6}{7}}$	α

perform a simulation based refinement. Alternatively, the Lyapunov function proposed in Cruz-Zavala and Moreno (2016) can be used to justify an initial setting.

5. Simulation experiments

In this section, three simulation experiments are carried out. For comparison, a function already proposed in the literature is considered in Section 5.1. Section 5.2 investigates the performance using randomly generated input signals f. The input signals have limited slew rate and it is demonstrated that the differentiator parameters have to be adapted accordingly during simulation. In Section 5.3 the order of the differentiator is increased such that the impact of noise is reduced.

5.1. *Simulation scenario 1*

Consider the function used in Levant (1998):

$$f(t) = \sin(t) + 5t + 0.001\cos(30t), \tag{67}$$

The second derivative w.r.t. time t has a maximum value of 1.9 at $t = \frac{3\pi}{2}$. Hence, according to equation (1) the Lipschitz constant $L = 1.9$. A RED with constant gains

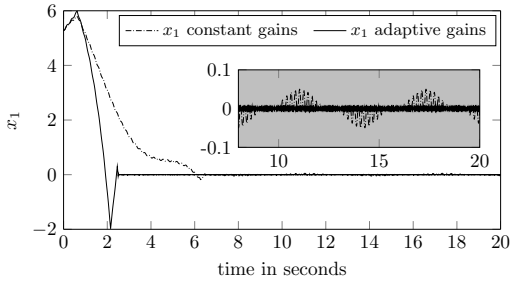

(a) Evolution of the error signal $x_1 = \frac{d}{dt}x - \hat{x}$.

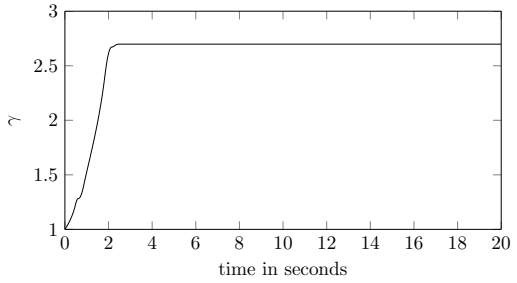

(b) Time behaviour of the adaptation parameter γ.

Figure 2.: Results of numerical simulation in order to compare the RED performance achieved by a constant gain setting and an adaptive gain implementation.

$\kappa_1 = 1.5$ and $\kappa_0 = 1.1$ is implemented in Matlab/Simulink[2]. This parameter setting corresponds to the roots $p_{1,2} = -0.75 \pm 0.7331j$ of the polynomial $\bar{w}(p)$ given in Theorem (2.1) and represents the well-established setting e.g. discussed in Y. Shtessel et al. (2014) for the case $L = 1$. Therefore, this implemented constant gains RED is not robust against the uncertainty term $\frac{d^2 f}{dt^2}$ in system (4) introduced by the considered signal (67). This also becomes evident in the simulation results shown in Figure 2 where the zoomed subplot reveals time instants at which the error x_1 can not be kept at zero. The performance of an adaptive gains RED also is depicted in Figure 2. The roots p_1 and p_2 are selected as used by the constant gains RED. In the adaptation law (37) $\alpha = 0.9\kappa_0$ was used. In order to obtain robustness the adaptation algorithm increases γ until $x_0 = 0$ is maintained, see Figure 2(b).

5.2. *Simulation scenario 2*

Randomly generated signals $f(t)$ with limited slew rate, see Figure 3(a), are considered. A uniformly distributed random signal of maximum absolute value 0.001 was also added to $f(t)$ in order to evaluate the proposed adaptive gains differentiator in the case of noisy input signals. The parameter setting of the differentiators was as in the first simulation scenario, however, its initial values were selected randomly from the interval $(0, 10)$. The time response of γ is shown in Figure 3(c), where the adaptation algorithm (42) with $\varepsilon = 0.001$ was implemented. Hence, γ is allowed to reduce. For experiments carried out with the same slew rate limitation, γ converges towards a similar range. The evolution of the estimation errors x_0 is depicted in Figure 3(b) which also includes zoomed plots indicating the achieved estimation accuracy. The depicted plots in Figure 3 also show results obtained with an input signal which has half of the slew rate as the other signals. It is interesting to see that this characteristic also can be observed in the behaviour of γ which settles at about half the value when compared to the other simulation experiments. Although not shown in the simulation results this dependency also can be observed in general, i.e. the multiplicity of bandwidth of the input signal is reflected in the "steady state value" of γ.

[2]A constant step size of 10^{-4}s was used during the simulation studies presented in this article. The initial values were selected as $z_0(0) = 5$ and $z_1(0) = 0.72$.

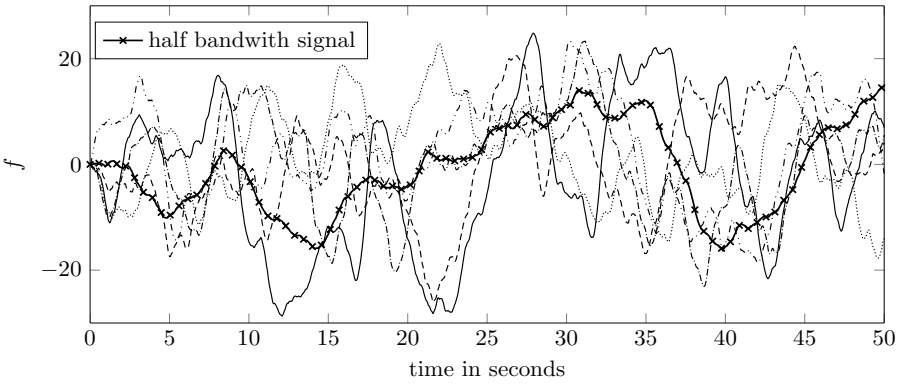

(a) Randomly generated signals $x(t)$ used to demonstrate the performance of the adaptive gains RED.

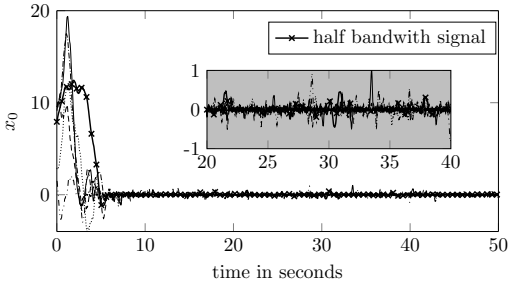

(b) Evolution of the estimation error x_0.

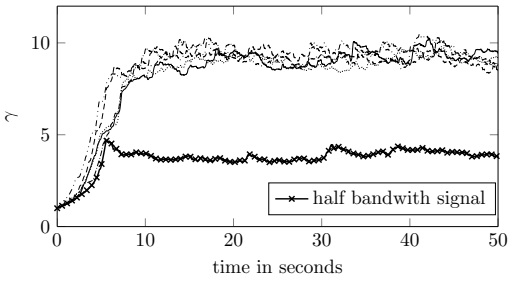

(c) Time behaviour of the adaptation parameter γ.

Figure 3.: Results of numerical simulation using randomly generated signals with limited slew rate. The estimation error x_0 vanishes for any tested input signal, the adapted parameter γ always converges towards a similar constant limit.

5.3. *Simulation scenario 3*

The input signal of the differentiator is assumed to be corrupted by noise of maximum amplitude ε and

$$f(t) = \sin(t) + \eta(t) \qquad \text{with} \qquad |\eta(t)| \leq \varepsilon \quad \forall t \geq 0, \tag{68}$$

hence a harmonic signal of frequency $1\frac{\text{rad}}{\text{s}}$ is applied as base signal. The function η representing the noise is implemented using a uniformly distributed random signal with $\varepsilon = 0.1$. The parameter α was selected as in the previous simulation scenarios, i.e. $\alpha = 0.9\kappa_0$. The adaptation algorithm as given in equation (42) was implemented in Matlab/Simulink. It is well known that the impact of noise may be reduced by increasing the order of the differentiator. In this simulation scenario, the first-time derivative of the input signal f as given in equation (68) is computed by a first order differentiator. Its parameters are computed according equation (18) using the roots $p_1 = -1.1$ and $p_2 = -1$. The performance achieved by this RED is compared to an estimate of an adaptive gains differentiator of order 4. The constant parameters κ_0, κ_1, κ_2, κ_3 and κ_4 are determined using the roots $p_1 = -1.1$ and $p_{2,3,4,5} = -1$ of the polynomial $\bar{w}(p)$ given in equation (56). Figure 4(a) shows the input signal f of the differentiators which is heavily affected by noise after 10 seconds. The error signals x_0 are plotted in Figure 4(b). Therein, it becomes evident that in case of the input signal

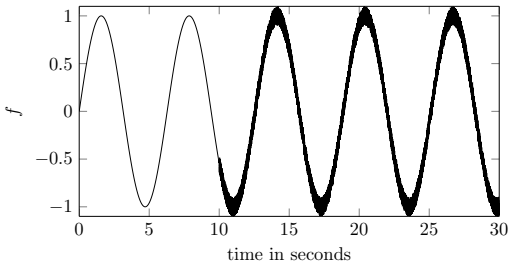

(a) Input signal f given in equation (68). Noise of maximum amplitude $\varepsilon = 0.1$ is added to the base signal $\sin(t)$ after 10 seconds.

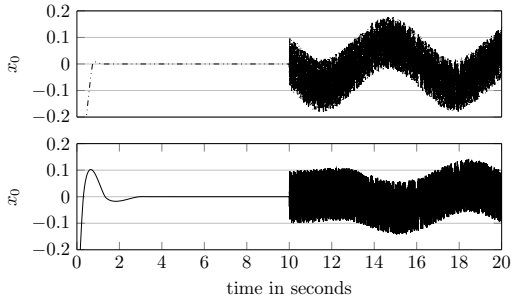

(b) Evolution of the estimation error x_0 of a first and a fourth order adaptive gains differentiator.

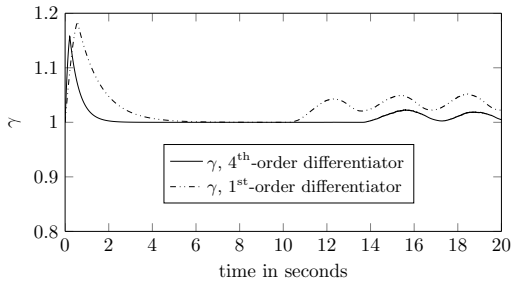

(c) Evolution of the adaptation parameter γ of generated by the first and the fourth order adaptive gains differentiator.

Figure 4.: Simulation results demonstrating the performance of higher-order differentiators in the presence of noisy input signals.

corrupted by noise, the maximum absolute value of the estimation error produced by the fourth order differentiator is less than that generated by the RED. The evolution of the adaptation parameter γ of both differentiators is shown in Figure 4(c). This simulation scenario is also used to compare the performance of the proposed adaptive gains algorithm with the existing algorithm discussed in Y. Shtessel et al. (2012). In this case, the adaptation law

$$\frac{d\kappa_0}{dt} = \begin{cases} \mu_1 \operatorname{sign}(|f - z_0| - \mu_2), & \text{if } \kappa_0 > \mu_4, \\ \mu_3, & \text{if } \kappa_0 \leq \mu_4, \end{cases} \tag{69a}$$

$$\kappa_1 = \mu_5 \kappa_0, \tag{69b}$$

with the positive constants μ_1, μ_2, μ_3, μ_4 and μ_5 is implemented. Hence, there are five parameters which have to be selected in order to adapt the two controller gains κ_0 and κ_1 of the differentiator. The parameter μ_2 is selected as 1.1ε which corresponds to the selection given in the adaptation algorithm (42). The parameter μ_3 indicates how fast the parameter κ_0 is increased if it shows its minimum value μ_4. The impact of the selected value of the parameter μ_3 to the overall dynamics seems not to be crucial and is selected as $\mu_3 = 1$. The parameters κ_0 and κ_1 are increased if $|f - z_0| > \mu_2$. The parameter μ_1, which is selected as 5.5, determines how fast this adaptation takes place. This also is the rate used to reduce the parameters in the case $|f - z_0| < \mu_2$. The parameter μ_4 may be regarded as a minimum gain of the differentiator. A "huge" value

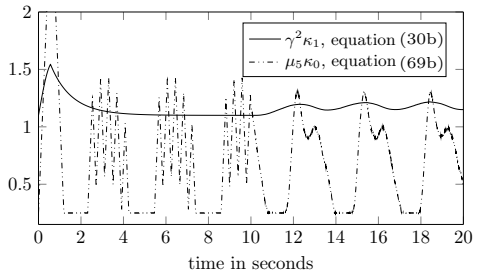

(a) Results obtained with $\mu_4 = 0.25$.

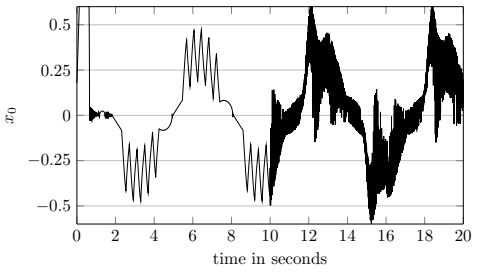

(b) Evolution of the estimation error x_0 achieved with gain adaptation according to equation (69).

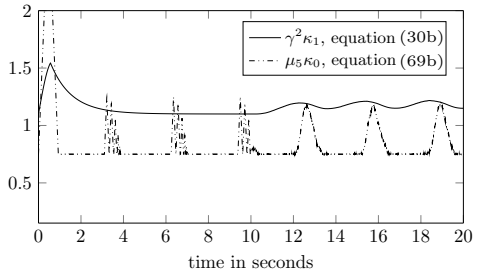

(c) Results obtained with $\mu_4 = 0.75$.

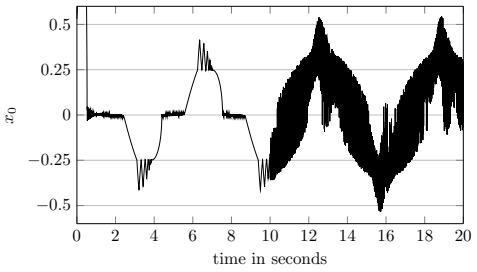

(d) Evolution of the estimation error x_0 achieved with gain adaptation according to equation (69).

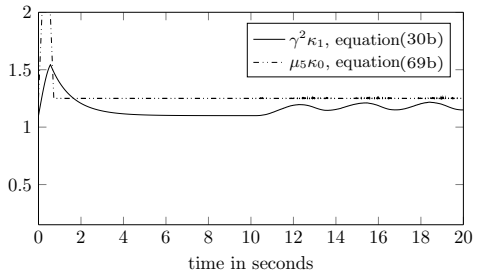

(e) Results obtained with $\mu_4 = 1.25$.

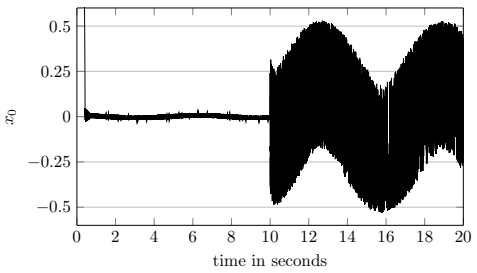

(f) Evolution of the estimation error x_0 achieved with gain adaptation according to equation (69).

Figure 5.: Comparison of the robust exact differentiators with adaptive gains.

of μ_4 yields high gains κ_0 and κ_1 and consequently there will be no adaptation required. Greater adaptation effort is required as the parameter μ_4 is reduced. This, however, impacts on the estimation accuracy. The discussed behaviour is illustrated in Figure 5 where three simulation results are shown. The parameter setting $\mu_4 = 0.25$, $\mu_4 = 0.75$ and $\mu = 1.25$ is used to obtain the results depicted in Figure 5(a) and 5(b), Figure 5(c) and 5(d) and Figure 5(e) and 5(f) respectively. The evolution of the estimation error x_0 obtained by the application of the proposed adaptation algorithm is shown in the upper plot in Figure 4(b).

6. Case study: Magnetic Levitation System

This section applies the adaptive gains differentiator to a magnetic levitation laboratory setup depicted in Figures 6(a) and 6(b). In Section 6.1 a brief system description and a dynamic model are given. A control law stabilizing the levitated ball is outlined

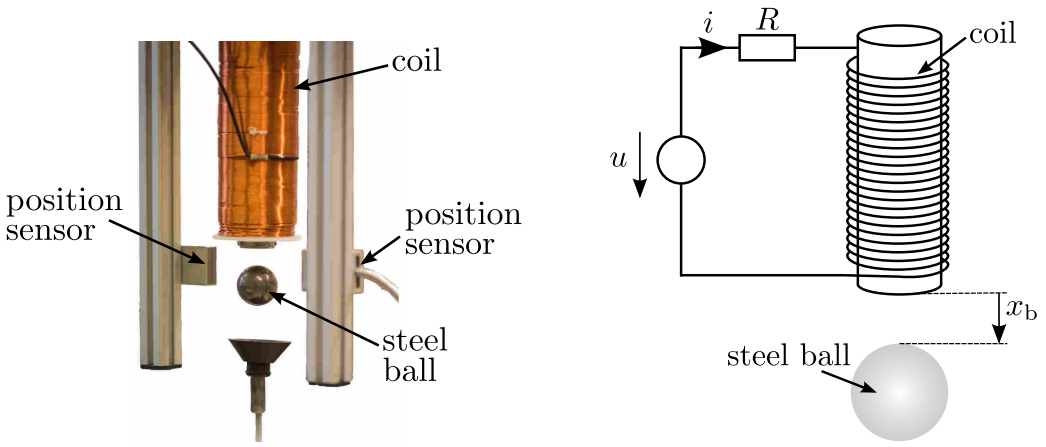

(a) Foto of the levitating ball system used for experiments.

(b) Schematic diagram of the setup.

Figure 6.: Photo and schematics of the laboratory magnetic levitated ball system.

in Section 6.2. The differentiator implementation is presented in Section 6.3. Results obtained from real world experiments are shown in Section 6.4.

6.1. *System description and modeling*

An electric current through the coil generates a magnetic field. The objective is to adjust this current such that the ball is levitated at a desired constant position r. It is well known that the dynamics can be modelled by

$$\frac{dx_\mathrm{b}}{dt} = x_\mathrm{v}, \tag{70a}$$

$$\frac{dx_\mathrm{v}}{dt} = g - \frac{c}{2m}\frac{i^2}{x_\mathrm{b}^2}, \tag{70b}$$

$$\frac{di}{dt} = -\frac{R}{L_0}i + \frac{c}{L_0}\frac{x_\mathrm{v} i}{x_\mathrm{b}^2} + \frac{1}{L_0}u, \tag{70c}$$

where x_b, x_v and i represent the distance between ball and coil, see Figure 6(b), the velocity of the ball and the electric current respectively. The electrical circuit consists of an ideal resistor (with resistance R), the coil (with inductance L_0) and a voltage source representing the system's input u. The acceleration of gravity is denoted by g, the mass of the ball is labelled as m and c is a positive constant related to the force acting on the ball due to the magnetic field[3]. The laboratory setup used in this paper provides measurements of the ball position x_b and the current i. The parameters of the laboratory setup are listed in Table 2.

6.2. *Design of a simple control law*

Although many sophisticated control techniques ensuring satisfactory tracking performance of the ball position are available a simple approach is implemented. A constant

[3]The dependency of the inductance L on the ball position x_1 is neglected in this model.

Table 2.: Parameters of the magnetic levitation system

parameter	value	unit
g	9.81	$\mathrm{m/s^2}$
m	$6.687 \cdot 10^{-3}$	kg
c	$1.05 \cdot 10^{-4}$	Hm
R	18	Ω
L_0	0.95	H

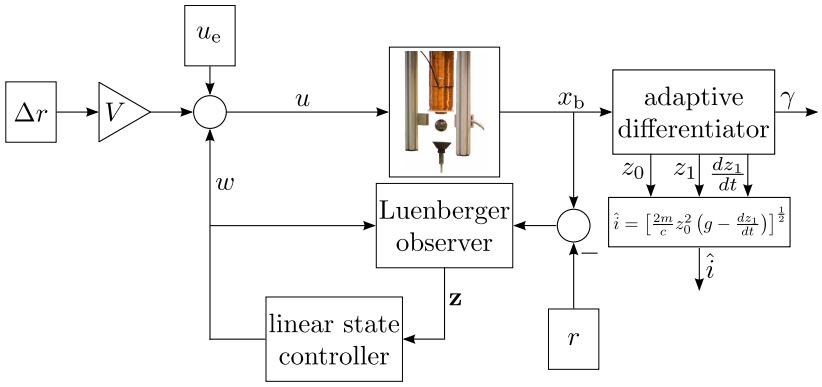

Figure 7.: Schematic diagram of the applied ball position control loop.

reference position r corresponds to the desired equilibrium point

$$\mathbf{x}_\mathrm{e} = \begin{bmatrix} r & 0 & r\sqrt{\frac{2mg}{c}} \end{bmatrix}^\mathrm{T}, \tag{71}$$

characterized by the constant input $u = u_\mathrm{e} = R\sqrt{\frac{2mg}{c}}r$, see system (70), which will be stabilized by a linear state controller. Denoting deviations from the desired equilibrium $\mathbf{x}_\mathrm{e}$ by $\mathbf{z}$ and deviations from the constant input u_e by w, i.e.

$$\mathbf{x} = \mathbf{x}_\mathrm{e} + \mathbf{z} \qquad \text{and} \qquad u = u_\mathrm{e} + w \tag{72}$$

a linear, time-invariant model approximating the the behavior of system (70) sufficiently close to the desired equilibrium $\mathbf{x}_\mathrm{e}$ is given by

$$\frac{d\mathbf{z}}{dt} = \begin{bmatrix} 0 & 1 & 0 \\ \frac{2\,g}{r} & 0 & -\frac{c\sqrt{2\frac{g\,m}{c}}}{m\,r} \\ 0 & \frac{c\sqrt{2\frac{g\,m}{c}}}{r\,L} & -\frac{R}{L} \end{bmatrix} \mathbf{z} + \begin{bmatrix} 0 \\ 0 \\ \frac{1}{L} \end{bmatrix} w. \tag{73}$$

The control law is executed at a constant sampling period of $\tau = 2\mathrm{ms}$. Therefore a linear, discrete-time state controller, which is based on a discretized version of system (73) is computed. It is designed such that all eigenvalues of the discrete-time closed-loop system are located at 0.89. A linear full-state discrete-time Luenberger observer based on the measured ball position is used to estimate the unmeasured ball velocity x_v and the current i for use by the controller. In order to deviate the ball position from its desired value r an additive reference signal Δr is considered as additional input which is weighted by the constant V, see Fig 7.

6.3. *Discrete-time Implementation of the adaptive gains differentiator*

The proposed adaptive gains differentiator is implemented in a discrete-time environment executed with a constant sampling time τ. A continuous-time differentiator as given in equation (47) in the case of constant gains, i.e. $\gamma = 1$, may be implemented in a discrete-time environment as

$$\begin{aligned} z_{i,k+1} &= z_{i,k} + \tau\kappa_i \left\lfloor x_{0,k} \right\rceil^{\frac{n-i}{n+1}} + \sum_{j=1}^{n-i} \frac{\tau^j}{j!} z_{j+i,k}, \\ z_{n,k+1} &= z_{n,k} + \tau\kappa_n \operatorname{sign}(x_{0,k}), \end{aligned} \tag{74}$$

which is proposed in Livne and Levant (2014). The idea of the applied discretization scheme is to preserve homogeneity properties of the continuous-time differentiation error dynamics Levant (2005). In this representation of the differentiator the notation $z_{i,k} := z_i(k\tau)$, $z_{i,k+1} := z_i((k+1)\tau)$ and $k = 0, 1, 2\ldots$ is used. A straightforward application of the mentioned discretization approach in the case of the adaptive gains differentiator given in (47) is given by

$$\begin{aligned} z_{i,k+1} &= z_{i,k} + \tau\gamma_k^{i+1}\kappa_i \left\lfloor x_{0,k} \right\rceil^{\frac{n-i}{n+1}} + \sum_{j=1}^{n-i} \frac{\tau^j}{j!} z_{j+i,k}, \\ z_{n,k+1} &= z_{n,k} + \tau\gamma_k^{n+1}\kappa_n \operatorname{sign}(x_{0,k}), \end{aligned} \tag{75}$$

where γ_k denotes $\gamma(k\tau)$ and results from

$$\gamma_{k+1} = \gamma_k + \frac{\alpha\,\tau}{2}\,\gamma_k \begin{cases} |x_{0,k}|^{-\frac{1}{2}} & \text{for} \quad |x_{0,k}| \geq 1 \\ |x_{0,k}| & \text{for} \quad |x_{0,k}| < 1 \\ \frac{1}{\gamma_k} - 1 & \text{for} \quad |x_{0,k}| < 1.1\varepsilon \end{cases} \qquad \text{with} \qquad \gamma_0 = 1, \tag{76}$$

which is a discrete-time realization of (42) based on Euler discretization.

6.4. *Experimental results*

A 4^{th} order adaptive gains differentiator as given by equations (75) and (76) was implemented. Note that this implementation is not part of the closed-loop control system. The sampling time was $\tau = 0.002$ seconds. The implemented differentiator is tuned such that the roots are located at

$$p_{1,2} = -0.25 \qquad \text{and} \qquad p_{3,4,5} = -0.5, \tag{77}$$

which yields parameters

$$\kappa_0 = 2, \quad \kappa_1 = 1.6, \quad \kappa_2 = 0.59, \quad \kappa_3 = 0.11, \quad \kappa_4 = 0.0078. \tag{78}$$

These parameters are chosen such that the estimation errors of a constant gains differentiator will not vanish, hence, adaptation is required in order to ensure estimation accuracy. The adaptation parameter α was selected as $\alpha = 0.9\kappa_0$ and ε was selected as 0.00001. Experimentally obtained results are shown in Figure 8. The measured ball position is plotted in Figure 8(a). In addition the outputs z_0 of a constant gains and

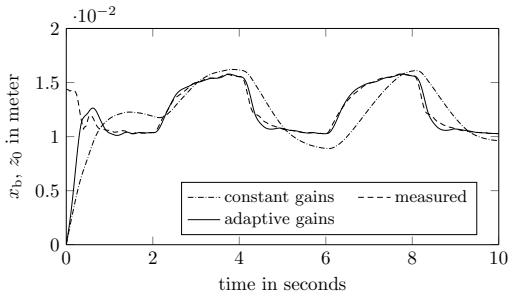

(a) Measured ball position x_1 and estimates z_0 obtained by a constant gains and an adaptive gains differentiator.

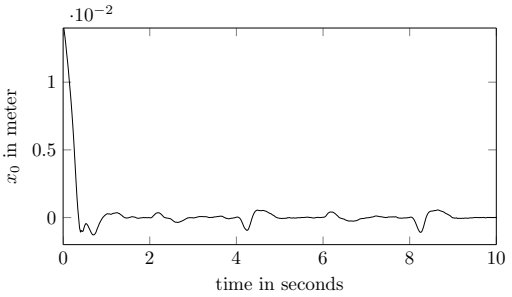

(b) Time evolution of the position error $x_0 = x - z_0$ of the adaptive gains differentiator.

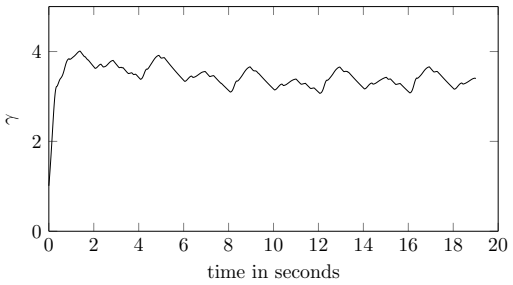

(c) Evolution of the adaptation parameter γ.

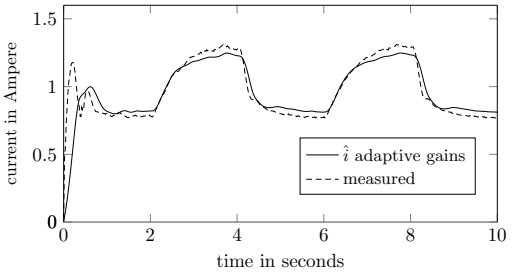

(d) Measured and estimated coil current required to lift the steel ball.

Figure 8.: Experimental results achieved with the magnetic levitated ball system depicted in Figure 6.

an adaptive gains differentiator using the parameters as listed in equation (78) are shown. It becomes evident that this differentiator gains are tuned such that the error x_0 does not vanish if no adaptation is implemented. The time evolution of the tuning parameter γ is depicted in Figure 8(c), the estimation error x_0 of the adaptive gains differentiator is shown in Figure 8(b). The parameter γ is increased initially and starts to oscillate at around 3.5 after achieving its resulting estimation accuracy. The estimation of the current i is depicted in Figure 8(d), where the estimate obtained by the adaptive gains differentiator is based on the re-arranged equation (70b), i.e.

$$\hat{i} = \left[\frac{2m}{c} z_0^2 \left(g - \frac{dz_1}{dt} \right) \right]^{\frac{1}{2}}, \tag{79}$$

where z_0 and z_1 where used as the estimate of the ball position x_b and velocity x_v respectively. Note that even the time derivative of the estimated ball velocity is required to compute the estimated current. This current estimate is compared to the estimation using the Luenberger observer and to the measured current, see Figure 8(d).

7. Conclusion

A new parameter tuning method for the first order robust exact differentiator has been established. By employing a pseudo-linear system perspective in the analysis, it has been possible to establish a general tuning heuristic to determine parameters for

arbitrary order differentiators. The method has been seen to lend itself to parameter adaptation. Both simulation experiments and a practical implementation case study have been used to demonstrate the paradigm. The method has great potential to bridge the gap between theory and practice by ensuring the gains of the differentiator are constantly adjusting to the characteristics of the signal to be differentiated.

References

Bacciotti, A., & Rosier, L. (2005). *Liapunov functions and stability in control theory* (2nd ed.). Springer-Verlag Berlin Heidelberg.

Banks, S. P., & Mhana, K. J. (1992). Optimal control and stabilization for nonlinear systems. *IMA Journal of Mathematical Control and Information*, *9*, 179-196.

Boyd, S., El Ghaoui, L., Feron, E., & Balakrishnan, V. (1994). *Linear matrix inequalities in system and control theory* (Vol. 15). Philadelphia, PA: SIAM.

Chawda, V., Celik, O., & O'Malley, M. (2011, June). Application of Levant's differentiator for velocity estimation and increased z-width in haptic interfaces. In *World haptics conference (whc), 2011 ieee* (p. 403-408).

Cruz-Zavala, E., & Moreno, J. A. (2016). Lyapunov functions for continuous and discontinuous differentiators. *IFAC-PapersOnLine*, *49*(18), 660 - 665. Retrieved from `http://www.sciencedirect.com/science/article/pii/S2405896316318213`

Cruz-Zavala, E., Moreno, J. A., & Fridman, L. M. (2011, Nov). Uniform robust exact differentiator. *IEEE Transactions on Automatic Control*, *56*(11), 2727-2733.

Davila, A., Moreno, J. A., & Fridman, L. M. (2009, Dec). Optimal lyapunov function selection for reaching time estimation of super twisting algorithm. In *48th ieee conference on decision and control.* (p. 8405-8410).

Kobayashi, S., & Furuta, F. (2007). Frequency characteristics of Levant's differentiator and adaptive sliding mode differentiator. *International Journal of Systems Science*, *38*(10), 825-832. Retrieved from `http://dx.doi.org/10.1080/00207720701631198`

Langson, W., & Alleyne, A. (1999). A stability result with application to nonlinear regulation: theory and experiments. In *Proceedings of the american control conference* (Vol. 5, p. 3051-3056 vol.5).

Langson, W., & Alleyne, A. (2002). A stability result with application to nonlinear regulation. *Journal of Dynamic Systems, Measurement, and Control*, *124*(3), 452-456.

Levant, A. (1998). Robust exact differentiation via sliding mode technique. *Automatica*, *34*(3), 379 - 384. Retrieved from `http://www.sciencedirect.com/science/article/pii/S0005109897002094`

Levant, A. (2003). Higher-order sliding modes, differentiation and output-feedback control. *International Journal of Control*, *76*(9-10), 924-941. Retrieved from `http://dx.doi.org/10.1080/0020717031000099029`

Levant, A. (2005). Homogeneity approach to high-order sliding mode design. *Automatica*, *41*(5), 823 - 830.

Livne, M., & Levant, A. (2014). Proper discretization of homogeneous differentiators. *Automatica*, *50*(8), 2007 - 2014.

Moreno, J. (2009, Jan). A linear framework for the robust stability analysis of a generalized super-twisting algorithm. In *6th international conference on electrical engineering, computing science and automatic control, cce* (p. 1-6).

Moreno, J., & Osorio, M. (2008, Dec). A Lyapunov approach to second-order sliding mode controllers and observers. In *47th ieee conference on decision and control* (p. 2856-2861).

Moreno, J., & Osorio, M. (2012, April). Strict Lyapunov functions for the super-twisting algorithm. *IEEE Transactions on Automatic Control*, *57*(4), 1035-1040.

Moreno, J. A. (2012). Sliding modes after the first decade of the 21st century. In L. Fridman, J. Moreno, & R. Iriarte (Eds.), (p. 113-149). Springer-Verlag Berlin Heidelberg.

Oliveira, T. R., Estrada, A., & Fridman, L. (2015, Dec). Global exact differentiator based on higher-order sliding modes and dynamic gains for globally stable output-feedback control. In *2015 54th ieee conference on decision and control (cdc)* (p. 4109-4114).

Oliveira, T. R., Estrada, A., & Fridman, L. (2016, June). Output-feedback generalization of variable gain super-twisting sliding mode control via global hosm differentiators. In *2016 14th international workshop on variable structure systems (vss)* (p. 257-262).

Orani, N., Pisano, A., & Usai, E. (2006, Dec). On a new sliding-mode differentiation scheme. In *Ieee international conference on industrial technology, 2006. icit 2006* (p. 2652-2657).

Orlov, Y. (2009). *Discontinuous systems: Lyapunov analysis and robust synthesis under uncertainty conditions*. Springer-Verlag London.

Orlov, Y., Aoustin, Y., & Chevallereau, C. (2011, March). Finite time stabilization of a perturbed double integrator - part i: Continuous sliding mode-based output feedback synthesis. *IEEE Transactions on Automatic Control*, *56*(3), 614-618.

Ortiz-Ricardez, F. A., Sanchez, T., & Moreno, J. A. (2015, Dec). Smooth Lyapunov function and gain design for a second order differentiator. In *54th ieee conference on decision and control (cdc)* (p. 5402-5407).

Pisano, A., & Usai, E. (2011). Sliding mode control: A survey with applications in math. *Mathematics and Computers in Simulation*, *81*(5), 954 - 979. Retrieved from `//www.sciencedirect.com/science/article/pii/S0378475410003095` (Important aspects on structural dynamical systems and their numerical computation)

Plestan, F., Shtessel, Y., Bregeault, V., & Poznyak, A. (2010). New methodologies for adaptive sliding mode control. *International Journal of Control*, *83*(9), 1907-1919. Retrieved from `http://dx.doi.org/10.1080/00207179.2010.501385`

Polyakov, A., & Poznyak, A. (2009, Aug). Reaching time estimation for super-twisting second order sliding mode controller via lyapunov function designing. *IEEE Transactions on Automatic Control*, *54*(8), 1951-1955.

Shtessel, Y., Edwards, C., Fridman, L., & Levant, A. (2014). *Sliding mode control and observation*. Birkhäuser, Springer Science+Business Media, New York.

Shtessel, Y., Taleb, M., & Plestan, F. (2012). A novel adaptive-gain supertwisting sliding mode controller: Methodology and application. *Automatica*, *48*(5), 759 - 769. Retrieved from `http://www.sciencedirect.com/science/article/pii/S0005109812000751`

Shtessel, Y. B., Moreno, J., Plestan, F., Fridman, L. M., & Poznyak, A. (2010, Dec). Super-twisting adaptive sliding mode control: A lyapunov design. In *49th ieee conference on decision and control (cdc)* (p. 5109-5113).

Sidhom, L., Pham, M. T., Thvenoux, F., & Gautier, M. (2010, July). Identification of a robot manipulator based on an adaptive higher order sliding modes differentia-

tor. In *International conference on advanced intelligent mechatronics, ieee/asme* (p. 1093-1098).

Sidhom, L., Smaoui, M., Thomasset, D., Brun, X., & Bideaux, E. (2011). Adaptive higher order sliding modes for two-dimensional derivative estimation. *18th IFAC World Congress*, *44*(1), 3063 - 3071. Retrieved from `http://www.sciencedirect.com/science/article/pii/S1474667016440814`

8. Appendices

Proof of Theorem 2.1

The eigenvalues of matrix $\mathbf{M}(x_0)$ are given in equation (16). Whenever p_1 and p_2 are selected such that $p^2 + \kappa_0 p + \kappa_1$ is a Hurwitz-polynomial, the eigenvalues satisfy $\Re\{s_k\} < 0 \quad \forall x_0(t) \quad k = 1, 2$. Consider the Lyapunov function

$$V(x_0, x_1) = p_1^2 \frac{1}{s_1^2(x_0)} + \frac{1}{2p_1p_2} x_1^2. \tag{80}$$

Its positive definiteness is ensured by $p_1p_2 > 0$, where the product $p_1p_2 \in \mathbb{R}$, and the relation $p_1^2 \frac{1}{s_1^2(x_0)} = p_1^2 \frac{1}{p_1^2 |x_0|^{-1}} = |x_0|$. Computing the time derivative of V given in equation (80) along the trajectories of system (13) yields

$$\frac{dV}{dt} = \left(1 + \frac{p_2}{p_1}\right) |x_0| s_1(x_0), \tag{81}$$

where $s_1^2 x_0 = p_1^2 |x_0|^{-1} x_0 = p_1^2 \operatorname{sign}(x_0)$ was exploited. Note that equation (81) is always real since $\left(1 + \frac{p_2}{p_1}\right) s_1(x_0) = -\kappa_0 |x_0|^{-\frac{1}{2}}$, where equation (18) is used, holds and consequently $\frac{dV}{dt} \leq 0$. From equation (16) negativeness of $\Re\{p_1\}$ and $\Re\{p_2\}$ ensure negative definiteness of the time-derivative of the Laypunov function. This motivates using the roots p_1 and p_2 for parameter tuning of the RED. The presented Lyapunov function is taken form Orlov et al. (2011). Applying the ideas of the extended invariance principle as outlined in Orlov (2009) ensures that the origin of system (13) in the unperturbed case is globally asymptotically stable. The finite convergence time from any bounded initial values $x_0(0)$ and $x_1(0)$ is guaranteed by the homogeneity properties of the system as in Levant (2005).

Proof of Theorem 2.2

Exploit the bounded real lemma which states that the statements 1. $||G(s)||_\infty < \frac{1}{L}$ and 2. LMI (9) is feasible, where $G(s) = \mathbf{c}^{\mathrm{T}} (s\mathbf{I} - \mathbf{A})^{-1} \mathbf{b}$, are equivalent, see Boyd, El Ghaoui, Feron, and Balakrishnan (1994). Using (10) yields

$$||G(s)||_\infty = \begin{cases} \frac{1}{\kappa_1} & \text{for} \quad \kappa_0^2 \geq 4\kappa_1 \\ \frac{4}{\kappa_0 \sqrt{8\kappa_1 - \kappa_0^2}} & \text{else.} \end{cases} \tag{82}$$

With the parameter selections κ_0 and κ_1 in the theorem, $||G(s)||_\infty = \frac{1}{\kappa_1}$ and from $\kappa_1 > L$, $||G(s)||_\infty = \frac{1}{\kappa_1} < \frac{1}{L}$ and consequently a feasible solution of the LMI (9) with some $\mathbf{P} > 0$ exists. LMI (9) is the result using

$$V(x_0, x_1) = \begin{bmatrix} \lfloor x_0 \rceil^{\frac{1}{2}} & x_1 \end{bmatrix} \mathbf{P} \begin{bmatrix} \lfloor x_0 \rceil^{\frac{1}{2}} \\ x_1 \end{bmatrix} =: \boldsymbol{\xi}^{\mathrm{T}} \mathbf{P} \boldsymbol{\xi} \tag{83}$$

as Lyapunov-function candidate[4], see J. Moreno and Osorio (2012); J. A. Moreno (2012). This can be shown from

$$\frac{d\boldsymbol{\xi}}{dt} = \frac{1}{2}\left|x_0\right|^{-\frac{1}{2}}\Big[\mathbf{A}\boldsymbol{\xi} + \Delta(x_0, \ddot{f})\mathbf{b}\Big], \tag{84}$$

where the functions

$$\Delta(x_0, \ddot{f}) := -2\left|x_0\right|^{\frac{1}{2}}\frac{d^2 f}{dt^2} \text{ and } \ddot{f} := f^{(2)} = \frac{d^2 f}{dt^2} \tag{85}$$

are introduced. The information on f given by (1) yields $\left(2\left|x_0\right|^{\frac{1}{2}}\right)^2\left(\frac{d^2 f}{dt^2}\right)^2 \leq \left(2\left|x_0\right|^{\frac{1}{2}}\right)^2 L^2$ which may be combined with (85) to give

$$\left(\lfloor x_0 \rceil^{\frac{1}{2}}\right)^2 L^2 - \Delta^2(x_0, \ddot{f}) \geq 0. \tag{86}$$

Inequality (86) with $\mathbf{n} := \begin{bmatrix}0 & 0\end{bmatrix}^{\mathrm{T}}$ may be written as

$$\begin{bmatrix}\boldsymbol{\xi}^{\mathrm{T}} & \Delta\end{bmatrix}\begin{bmatrix}\mathbf{c}L^2\mathbf{c}^{\mathrm{T}} & \mathbf{n} \\ 0 & -1\end{bmatrix}\begin{bmatrix}\boldsymbol{\xi} \\ \Delta\end{bmatrix} \geq 0, \tag{87}$$

Introducing the scaling

$$\frac{1}{\left|x_0\right|^{\frac{1}{2}}}\begin{bmatrix}\boldsymbol{\xi}^{\mathrm{T}} & \Delta\end{bmatrix}\begin{bmatrix}\mathbf{c}\mathbf{c}^{\mathrm{T}} & \mathbf{n}_{2\times 1} \\ 0 & -1\end{bmatrix}\begin{bmatrix}\boldsymbol{\xi} \\ \Delta\end{bmatrix} \geq 0 \tag{88}$$

and combining with the time derivative of the Lyapunov function V along the trajectories of system (4) yields

$$\frac{dV}{dt} \leq \frac{1}{2\left|x_0\right|^{\frac{1}{2}}}\begin{bmatrix}\boldsymbol{\xi}^{\mathrm{T}} & \Delta\end{bmatrix}\begin{bmatrix}\mathbf{A}^{\mathrm{T}}\mathbf{P} + \mathbf{P}\mathbf{A} + \mathbf{c}L^2\mathbf{c}^{\mathrm{T}} & \mathbf{P}\mathbf{b} \\ \mathbf{b}^{\mathrm{T}}\mathbf{P} & -1\end{bmatrix}\begin{bmatrix}\boldsymbol{\xi} \\ \Delta\end{bmatrix}, \tag{89}$$

Whenever the matrix inequality (9) has a feasible solution, the time derivative of the Lyapunov function V in (89) is negative definite. Applying the quasihomogeneity principle from Orlov (2009), system (4) is homogeneous of degree -1 w.r.t. the homogeneity dilation $\delta_\varepsilon : (x_0, x_1) \mapsto \left(\varepsilon^2 x_0, \varepsilon x_1\right)$ and parameter $\varepsilon > 0$, the origin of the system (4) is globally finite-time stable.

Proof of Theorem 2.3

Select $\kappa_1 = \gamma L$ with $\gamma > 1$ to ensure the desired equilibrium point at $x_0 = x_1 = 0$. Using inequality (23)

$$\kappa_0^4 - 8\gamma L\kappa_0^2 + 16L^2 < 0$$

κ_0 is selected such that the above holds. Using $\kappa_0^4 - 8\gamma L\kappa_0^2 + 16L^2 = 0$ yields

$$\kappa_0 = 2\sqrt{L}\sqrt{\gamma - \sqrt{\gamma^2 - 1}} \tag{90}$$

[4]This Lyapunov-function does not satisfy the properties typically required of Lyapunov-functions. A detailed discussion of this is presented in J. Moreno and Osorio (2012) and references therein.

These results determine an interval for the selection of κ_0 such that the roots p_1 and p_2 are complex and in addition inequality (23) is satisfied. The parameter κ_0 has to be selected as $\kappa_0 < 2\sqrt{\kappa_1}$ so that the roots are complex and $\kappa_0 > 2\sqrt{L}\sqrt{\gamma - \sqrt{\gamma^2 - 1}}$. The result follows directly.